Acta Tropica 233 (2022) 106585

Contents lists available at ScienceDirect

Acta Tropica

journal homepage: www.elsevier.com/locate/actatropica

Unsupervised machine learning and geometric morphometrics as tools for the identification of inter and intraspecific variations in the Anopheles Maculipennis complex

Nicolò Bellin [a,*], Mattia Calzolari [b], Giulia Magoga [c], Emanuele Callegari [b], Paolo Bonilauri [b], Davide Lelli [b], Michele Dottori [b], Matteo Montagna [c], Valeria Rossi [a]

[a] University of Parma, Department of Chemistry, Life Sciences and Environmental Sustainability, Parco Area delle Scienze, 11/A 43124 Parma, Italy
[b] Istituto Zooprofilattico Sperimentale della Lombardia e dell'Emilia Romagna "B. Ubertini'' (IZSLER), Brescia, Italy
[c] Università degli Studi di Milano, Dipartimento di Scienze Agrarie e Ambientali, Via Celoria 2, Milan 20133, Italy

ARTICLE INFO

Keywords:
Anopheles maculipennis s.s.
Anopheles daciae sp. inq.
UMAP
HDBSCAN
Wing phenotypic plasticity
COI haplotypes

ABSTRACT

Geometric morphometric analysis was combined with two different unsupervised machine learning algorithms, UMAP and HDBSCAN, to visualize morphological differences in wing shape among and within four Anopheles sibling species (*An. atroparvus*, *An. melanoon, An. maculipennis* s.s. and *An. daciae* sp. inq.) of the Maculipennis complex in Northern Italy. Specifically, we evaluated: (1) wing shape variation among and within species; (2) the consistencies between groups of *An. maculipennis* s.s. and *An. daciae* sp. inq. identified based on COI sequences and wing shape variability; and (3) the spatial and temporal distribution of different morphotypes. UMAP detected at least 13 main patterns of variation in wing shape among the four analyzed species and mapped intraspecific morphological variations. The relationship between the most abundant COI haplotypes of *An. daciae* sp. inq. and shape ordination/variation was not significant. However, morphological variation within haplotypes was reported. HDBSCAN also recognized different clusters of morphotypes within *An. daciae* sp. inq. (12) and *An. maculipennis* s.s. (4). All morphotypes shared a similar pattern of variation in the subcostal vein, in the anal vein and in the radio-medial cross-vein of the wing. On the contrary, the marginal part of the wings remained unchanged in all clusters of both species. Any spatial-temporal significant difference was observed in the frequency of the identified morphotypes. Our study demonstrated that machine learning algorithms are a useful tool combined with geometric morphometrics and suggest to deepen the analysis of inter and intra specific shape variability to evaluate evolutionary constrains related to wing functionality.

1. Introduction

The occurrence of cryptic sibling-species (morphologically similar but genetically distinct species) is far more common than previously thought (Pfenninger and Schwenk, 2007). On the other hand, due to phenotypic plasticity, i.e. the ability of a genotype to produce different phenotypes in response to environmental stimuli, conspecific specimens may be assigned to different taxa (DeWitt and Scheiner, 2004; West--Eberhard, 2005; Sommer, 2020). Moreover, populations adapted to local conditions, which are ecotypes, show specialization and geographic variation within species, responsible for generating a range of phenotypes in response to different environmental cues (Begon et al., 2006). Ecotypes are the result of the strict interaction between genetic heritage and specific environments. The distinction between local ecotypes and polymorphic populations is not always clear and easy to identify. Molecular methods greatly improve our ability to recognize cryptic species, phenotypic plasticity and ecotypes but the results can in some cases be biased due to, for instance, incomplete sampling (in time and space) or the markers used (Vrijenhoek et al., 2009; Magoga et al., 2021) .

The occurrence of cryptic sibling-species, phenotypic plasticity and ecotypes may lead to significant problems in surveillance and control when morphologically similar species differ in vector capacity due to differences in their ecology, ethology and thus in the propensity to bite humans (Gildenhard et al., 2019; Francuski et al., 2019; Kareemi et al., 2021).

* Corresponding author.
E-mail address: nicolo.bellin@unipr.it (N. Bellin).

https://doi.org/10.1016/j.actatropica.2022.106585
Received 18 May 2022; Received in revised form 8 June 2022; Accepted 30 June 2022
Available online 3 July 2022

The *Anopheles* genus includes more than 480 species, 70 of which are known to transmit malaria (Manguin et al., 2008). The genus includes several complexes of species, often indistinguishable at morphological level, and with different vectorial capacity (Manguin et al., 2010). The most dangerous vectors of malaria in the Holarctic region belong to the *Anopheles maculipennis* complex (hereafter Maculipennis complex). Among the 22 species in this group, *Anopheles messeae* is the most widely spread and genetically diverse species in Eurasia (Bertola et al., 2022). Recently, a new taxon close to *Anopheles messeae* named *Anopheles daciae* was defined based on ITS2 polymorphisms (Nicolescu et al., 2004; Lilja et al., 2020), but it taxonomic status is still under debate (Artemov et al., 2021), so we refer to this taxon as *Anopheles daciae* species inquirenda (sp. inq.).

In Northern Italy, the distribution of the species belonging to the Maculipennis complex was recently updated by extensive field sampling, during which the following four species were identified: *Anopheles atroparvus, Anopheles melanoon, Anopheles maculipennis* sensu stricto (s. s.) *and Anopheles daciae* species inquirenda (sp. inq.; Calzolari et al., 2021). In Calzolari et al. (under revision), some very distinct and monophyletic groups of individuals (based on the COI gene) were identified in this area. Specifically, two groups within *An. maculipennis* s. s. and two within *An. daciae* sp. inq. were recognized. In a complementary study, a machine learning algorithm, support-vector machine (SVM), integrated into geometric morphometric analysis, was used for the discrimination of two sibling species of the Maculipennis complex (Bellin et al., 2021). This analysis correctly classified 83% of *An. maculipennis* s.s. and 79% of *An. daciae* sp. inq. and revealed a clear differentiation in mean wing shape (Bellin et al., 2021). In particular, three main landmarks (11, 15 and 16) were identified on the wing as the most important in species recognition within the complex (Fig. 1). Landmark 11 is linked to the shape of the anal vein and is a trait used to discriminate between two different mosquito genera (*Uranotaenia* and *Culex*) (Severini et al., 2009; Becker et al., 2010). Landmarks 15 and 16, in the center of the wing, are the extremities of the radiomedial veins and are used as discriminative traits in identification of species of the *Culiseta* genus (Severini et al., 2009; Becker et al., 2010).

In this study, geometric morphometric analysis was combined with unsupervised machine learning techniques (UMAP and HDBSCAN) to investigate the variation in wing shape in individuals belonging to the four species of the Maculipennis complex in Northern Italy. Specifically, we aim to distinguish between phenotypic plasticity and ecotypes by evaluating: (1) wing shape variation among and within species; (2) the morphometric analytic support of inter group consistencies of *An. maculipennis* s.s. and *An. daciae* sp. inq. identified based on genetic information (Calzolari et al. under revision) and the variability of wing shape; and (3) the spatial and temporal distribution of different morphotypes of *An. maculipennis* s.s. and *An. daciae* sp. inq.

2. Materials and methods

2.1. Study area

The surveyed area included the plain areas in Emilia-Romagna and Lombardy, two densely populated regions of Northern Italy, with 14.5 million people. We sampled mainly in the Po Valley area of the two regions, the most suitable environment for mosquitoes, featured by vast

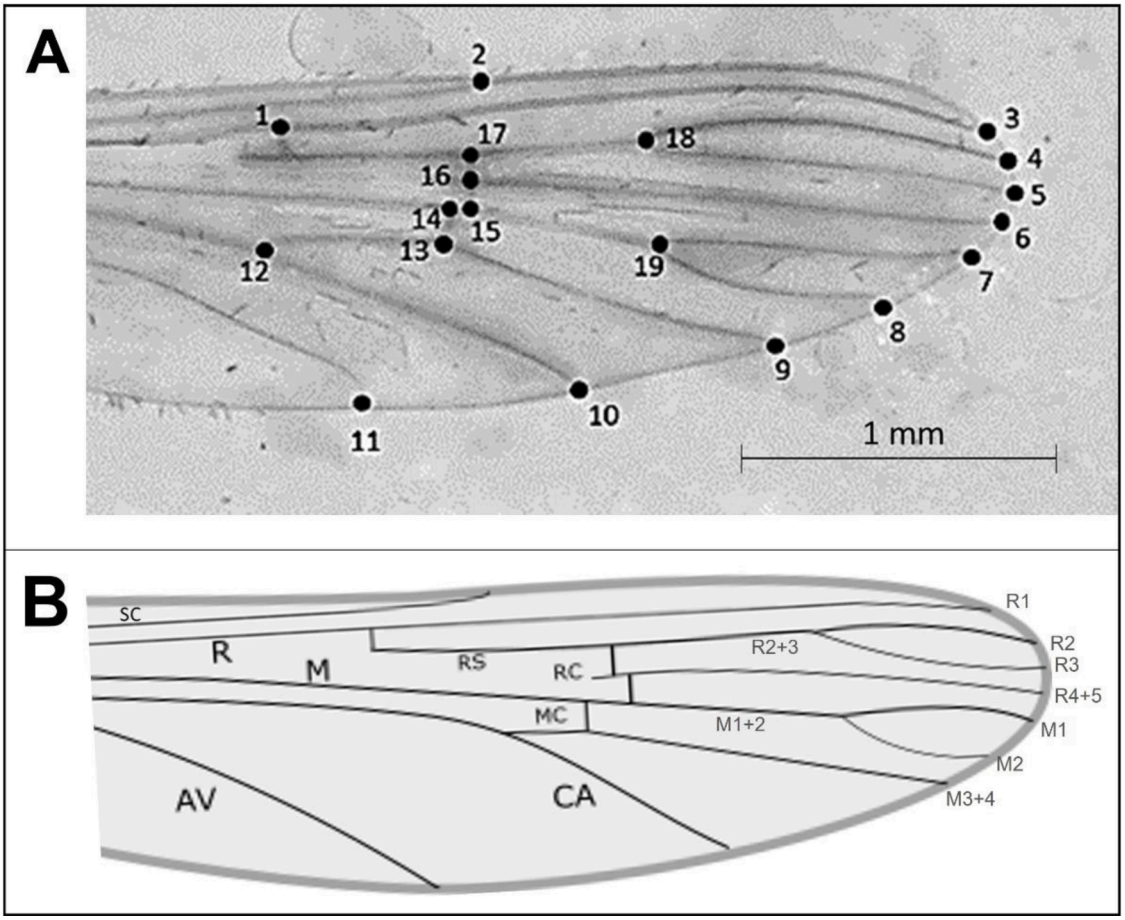

Fig. 1. In panel A right wing of an *An. daciae* sp. inq. female with the 19 landmarks. In panel B right wing representation with depicted the principal veins: subcostal (SC), radius (R), radius 1 (R1), radius 2 (R2), radius 3 (R3), radius 2 + 3 (R2+3), radius 4 + 5 (R4+5), radial sector (RS), radiomedial (RC), media (M), media 1 (M1), media 2 (M2), media 2 + 3 (M2+3), media 3 + 4 (M3+4) mediocubital (MC), cubitus anterior (CA), anal (AV).

areas of agricultural land, often interspersed with industrial-urban areas. The agricultural land is predominantly cropland with fields sometimes bordered by green strips, few and scattered trees and a dense irrigation network. Natural areas are rare, consisting mainly of river banks, characterized by riparian vegetation, or protected and re-naturalized areas. The surveyed area features a wide variety of breeding sites suitable for *Anopheles* mosquitoes, such as rice fields (e.g. Lomellina area) or the wetlands near the Po river delta, one of the largest wetland areas in Europe (Valli di Comacchio and Po River Delta).

2.2. Mosquitoes sampling and genetic data generation

In 2017 and 2018, we collected mosquitoes using manual aspirators in farms or adult overwintering sites at 43 sites and using carbon dioxide-baited traps at 103 sites included in the WNV surveillance plans (Calzolari et al., 2021). Manual aspirations were performed on farms with a variety of animals (cattle, horses, goats and poultry), suitable for the collection of engorged and host-seeking mosquitoes, and in uninhabited buildings, suitable for the collection of overwintering mosquitoes.

From each collected specimen, the internal transcribed spacer 2 (ITS2) was PCR amplified using as a template the DNA extracted from a single leg; the PCR amplicons were then sequenced to identify the individual species (data from Calzolari et al., 2021). To investigate the intraspecific genetic variability and its congruence with intraspecific wing shape variation, a fragment of the mitochondrial COI was PCR amplified (Calzolari et al., 2021) for a subset of randomly selected individuals belonging to *An. maculipennis* s.s. and *An. daciae* sp. inq. The COI sequences obtained were aligned using MUSCLE (Edgar 2004) with the default parameters and then the different haplotypes were identified using R version 3.6.2 (R Core Team, 2019) and the library *haplotypes* (https://biolsystematics.wordpress.com/r/). The morphometric analyses considered only haplotypes consisting of more than five individuals. K2P (Kimura, 1980) nucleotide distances were estimated between the selected haplotypes using the library *ape* (Popescu et al., 2012), as in Magoga et al. (2018).

According to the ITS2 sequences, the four following species were identified: *An. daciae* sp. inq. (322), *An. maculipennis* s.s. (124), *An. atroparvus* (10), and *An. melanoon* (4) (Calzolari et al., 2021; Bellin et al., 2021). Haplotype diversity within species was computed using the Shannon-Wiener diversity index (Shannon and Wiener, 1963).

2.3. Inter-specific diversity of wing shape in embedding space (UMAP)

For geometric morphometric analysis, the right wing of each female was dissected and mounted as reported in Bellin et al. (2021). To obtain a set of coordinates, scaled to unit-centroid size and rotated using a least-squares criterion, for each specimen, the landmarks were standardized using the Generalized Procrustes Analysis (GPA) (Bookstein, 1991; Goodal, 1991, 1996; Klingenberg, 2013; Tatsuta et al., 2018). This new data set was further processed with a dimensionality reduction algorithm (UMAP) (McInnes et al., 2018) that reduced the dimension of the dataset from 38 dimensions (19 pairs of landmarks coordinates, x and y) to two dimensions (UMAP 1 and UMAP 2). The UMAP algorithm is driven by two important hyperparameters: the first is the number of neighbors, which evaluates how the algorithm balances the local versus global structure of the data. Low neighbor values force UMAP to capture local structure, while high values capture global structures, losing finer and local relationships. To obtain a good global interspecific representation of the shape of the Maculipennis complex's, a neighbor value of 70 was set. The second hyperparameter is the minimum distance among neighbors: this evaluated how tightly similar points are grouped in the embedding. Low values result in clumpier embedding. To highlight differences among groups of species a distance value of 0 was set. The species identity information obtained from DNA barcoding analysis was superimposed on UMAP. To get a general idea of the wing shape variation represented by UMAP embedding, an inverse transformation approach was used. A convex hull that encompasses the embedding space was drawn and a grid of 13 points equispaced in the convex hull area were sampled. The sampled points were inverse transformed to obtain the representation of 13 wing shapes. Using wireframe graphs, the sub sample of wing shapes obtained by the inverse transformation was superimposed and compared with the mean shape of the Maculipennis complex. The Generalized Procrustes Analysis (GPA) was performed with the R package geomorph (Adams et al., 2020). UMAP analysis was performed in the Python umap library (https://github.com/lmcinnes/umap).

2.4. Intra-specific diversity of wing shape in An. maculipennis s.s. and An. daciae sp. inq

To find possible relationship between shapes and genetic markers and to capture local representations of the data, UMAP embedding was computed for *An. maculipennis* s.s. and *An. daciae* sp. inq. For this purpose, the first hyperparameter (number of neighbors) was set to a value of 15 while the second hyperparameter (minimum distance) was maintained at 0. For each species, the genetic information of the COI groups obtained from DNA barcoding analysis was superimposed on each UMAP embedding. To test differences in wing shapes of individuals belonging to the two different groups identified based on the COI gene tree, a PERMANOVA test was performed on shapes coordinates with 999 permutations (Anderson, 2001). The correlation between K2P nucleotide distance (Kimura, 1980) among the identified haplotypes and the mean wing shape of each haplotype was computed by Mantel test using Spearman's method and 999 permutations.

To identify different intraspecific wing morphotypes, an unsupervised clustering method was used that considered hierarchical estimates, Hierarchical Density-Based Spatial Clustering (HDBSCAN) algorithm (Campello et al., 2013). Clustering organized the data into a finite set of categories. In the density-based clustering paradigm, clusters are defined as dense areas separated by sparse regions. HDBSCAN outperforms others density clustering algorithms as it separates points that belong to clusters with outliers. The algorithm also assigns a soft partition value expressed as probability; for each observation, the probability is proportional to its membership (probability of belonging a particular cluster). HDBSCAN is driven by two main hyper parameters: min_cluster_size and min_samples. To find the best combination of HDBSCAN hyper parameters, a randomized grid search procedure was used. Along the two hyperparameters ranges, different values were randomly sampled. The best couple was selected according to the maximization of a validity measure (DBCV) proposed by a clustering density approach (Moulavi et al., 2014). HDBSCAN clustering analysis was performed in the Python hdbscan library (https://github.com/scikit-learn-contrib/hdbscan) and scikit-learn library (https://scikit-learn.org/stable/about.html). For both *Anopheles* species, the mean shape of different morphotypes was compared by PERMANOVA test with 999 permutations and considering the residual randomization. The mean shapes of different morphotypes were compared by a pairwise post-hoc test based on Euclidean distance. To visualize landmark pattern variation among intraspecific morphotypes, the cluster's mean shape was superimposed on the mean shape of each taxon by wireframe graph.

To test intraspecific spatial-temporal differences in morphotype abundance, a GLMM model was used with Poisson family function and with a maximum likelihood method (Laplace approximation). The model accounted for random and fixed effects. The random effects included a nested temporal structure for sampling dates (day in month) and a nested spatial structure for sampling sites (locality in province). The estimated intercept varied between crossed random effects (month and province). The fixed effect included the type of trap used to capture the specimens (CO_2 or manual), the morphotype and the interaction among factors. GLMM models were computed by R package lme4 (Bates et al., 2015).

3. Results

3.1. Inter-specific diversity in embedding space (UMAP)

By analyzing 460 wings, one for each of the 460 molecularly identified individuals (322 *An. daciae* sp. inq., 124 *An. maculipennis* s.s., 10 *An. atroparvus* and 4 *An. melanoon*), in the embedding space generated by UMAP, *An. melanoon* clustered separately from *An. atroparvus* specimens along UMAP 2: the first at the bottom and the second at the top (Fig. 2 panel A). Most *An. maculipennis* s.s. specimens were arranged in the top-left of the plot, with other specimens spread along the maps. *An. daciae* sp. inq. specimens showed the highest dispersion, with a major concentration of specimens in the bottom-right region of the maps. The wireframe graphs obtained by UMAP inverse transformation showed the 13 main pattern variations in wing shape among species within the Maculipennis complex (Fig. 2 panel B). Differences in *An. atroparvus* and *An. melanoon* were clearly shown by the distance between the centroids (Fig. 2 panel A) and the wing shapes 3 and 13, respectively (Fig. 2 panel B). The pattern of differentiation is less clear between *An. daciae* sp. inq. and *An. maculipennis* s.s. considering the centroids and, most of all, the continuum of different shapes.

3.2. Intra-specific diversity of An. daciae sp. inq. and An. maculipennis s.s

The 166 *An. daciae* sp. inq. and 80 *An. maculipennis* s.s. individuals analyzed in this study were found to belong to 77 and 45 haplotypes, respectively, based on COI gene (Table 1). The three most abundant haplotypes were identified within *An. daciae* sp. inq. COI group A (Calzolari et al. under revision), namely h2, h27 and h11, which included 23, 14, 10 individuals, respectively. Within *An. daciae* sp. inq. COI group B, the two most abundant haplotypes were h20 and h15, including 7 and 6 individuals, respectively. For *An. maculipennis* s.s. COI group 1 (Calzolari et al. under revision) only one abundant haplotype (h1) was detected, including 8 individuals, while in COI group 2, no haplotype including more than 5 individuals was found. Haplotype diversity (Shannon-Wiener index) was very similar in *An. daciae* sp. inq. (3.80) and *in An. maculipennis* s.s. (3.59).

For both the most abundant taxon (*An. daciae* sp. inq. and *An. maculipennis* s.s.), the superimposition of COI groups and haplotypes did not support the correlation between COI information and shape ordination (Fig. 3). This result was confirmed by PERMANOVA test (Tables 2 and S1) and the correlation between haplotype COI nucleotide distance and haplotype shape difference was not significant (Mantel statistic: 0.049 and *p*-value: 0.44).

The best set of HDBSCAN's hyperparameters was min_cluster_size = 5 and min_samples = 5 for both *An. daciae* sp. inq. and *An. maculipennis* s.s. with a cluster validity metric (DBCV) values of 0.12 and 0.20, respectively. HDBSCAN identifies 12 morphotypes for *An. daciae* sp. inq. and 4 morphotypes for *An. maculipennis* s.s. (Fig. 4). In both taxa, the MANOVA test revealed a significant difference in wing shape among morphotypes. All pairwise comparisons between morphotypes were significant (Table S2).

In *An. daciae* sp. inq., the most frequent pattern of variation from the mean shape involved landmark 2 (in 7 out 12 clusters), located in the subcostal vein, and landmark 11, located in the anal vein (in 7 out of 12 clusters) (Figs. 1 and 5). Other frequent patterns of variation observed involved the radio medial cross veins (landmarks 15, 16 and 17) and the cubitus veins (landmark 10) (Figs. 1 and 5). Cluster C did not diverge from the mean shape of the species. The highest difference in variation was observed for cluster D. In *An. maculipennis* s.s., the most frequent pattern of variation from the mean shape involved landmark 2, 10, 11 and 16 (in 2 out of 4 clusters). Another pattern of variation was observed in the radio medial cross veins (landmarks 15 and 17), in the medio cubital cross vein (landmark 12) and in the bifurcation of the radius vein (R_{2+3}) (landmark 18). The landmarks from 4 to 8, located in the marginal part of the wings, did not change in any clusters for both taxa.

Considering the capture techniques, morphotype abundance did not show significant intraspecific spatial-temporal differences (Table S3).

4. Discussion

We used a combined machine learning and geometric morphometric approach which was useful to investigate shape variation when taxa are difficult to discern using standard taxonomic approaches (Lorenz et al., 2012, 2015a, 2015b; Wilke et al., 2016). In order to investigate the relationship between wing shape and genetic markers, and to capture intraspecific differentiation of the four sibling species of the Maculipennis complex, we combined the geometric morphometric approach with the unsupervised machine learning algorithms UMAP and HDBSCAN.

As reported in Bellin et al. (2021), the use of machine learning improved the use of geometric morphometrics and allowed us to describe and recognize variability patterns among and within sibling species.

In the analysis of shape, especially in sibling species, the combined approach of UMAP and geometric morphometrics is unusual. Unlike PCA and most common eigenvector analysis, UMAP was able to capture data nonlinearity (Yang et al., 2021). In a previous study, carried out on the same data set, we showed that the first two PCs explained only 33% of the total variance and appeared not very useful for discriminating among all species of the complex as well as *An. maculipennis* s.s. from *An. daciae* sp. inq. (Bellin et al., 2021). The correct classification of 83% *An. maculipennis* s.s. and 79% of *An. daciae* sp. inq. was obtained by the integration of geometric morphometric analysis and a supervised machine learning algorithm such as the support-vector machine (Bellin et al., 2021). Here, we showed that UMAP, an unsupervised machine learning algorithm, allowed us to describe the wing shape variation patterns among the four sibling species of Maculipennis complex, namely *An. atroparvus, An. melanoon, An. maculipennis* s.s., and *An. daciae* sp. inq. In addition, it mapped the morphological variation within species. UMAP dimensionality reduction did not allow a clear distinction between morphotypes of An. maculipennis s.s. and *An. daciae* sp. inq. and confirmed that several specimens of both taxa were not completely split in the UMAP embedding. However, the centroids position might indicate evolutionary trajectories that have differentiated the species. UMAP algorithm was used in *Saccharomyces cerevisiae* to identify groups of genes related to protein structures, protein complexes and pathways (Dorrity et al., 2020) and to find fine-scale relationships and cryptic structures in the geography, genotypes and phenotypes in human populations (Diaz-Papkovich et al., 2019). This procedure should be tested in other complex or cryptic species to verify its effectiveness and generalizability.

In this study, UMAP allowed us to describe the occurrence of discontinuous wing shape morphotypes in the four analyzed species and highlighted the great inter and intra specific variability of the Maculipennis complex. COI mtDNA region is often used as barcoding region for species identification but also for a first assessment of the genetic population structure (e.g., Brunetti et al., 2019; Zheng et al., 2019; Doorenweerd et al., 2020). Due to the intraspecific variability of the COI we found in *An. daciae* sp. inq and in *An. maculipennis* s.s., it was interesting to investigate the morphological variability of COI haplotypes also considering that this mitochondrial marker is mostly used, sometimes in association with others, in integrated taxonomic studies. Within the two most abundant taxa (*An. daciae* sp. inq. and *An. maculipennis* s.s.), two different groups and several haplotypes were described based on COI sequences. The number of haplotypes is higher in *An. daciae* sp. *inq* than in *An. maculipennis* s.s. but the diversity index is very similar in the two species. However, UMAP ordination and statistical tests indicated that the correlation between COI variation and shape ordination/variation was not significant. This result is not surprising because as well as other possible factors, wing shape is a

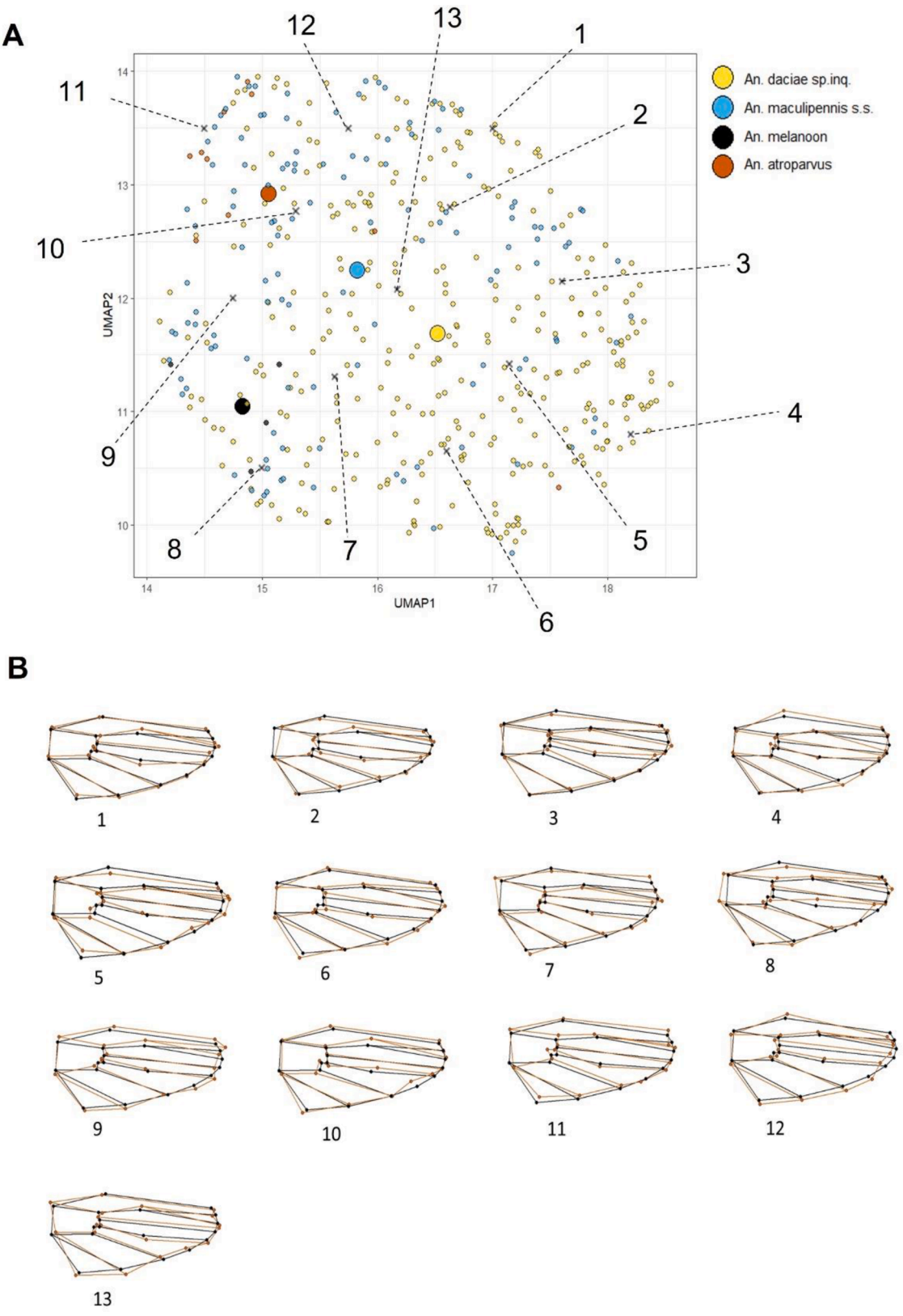

Fig. 2. A. UMAP embedding space relative to the four species wing shapes (*An. daciae* sp. inq., *An. maculipennis* s.s., *An. melanoon* and *An. atroparvus*) of the Maculipennis complex; the species centroid (greater size points) and the position of equispaced sampled points in the convex hull were reported; dashed lines and numbers indicate the wing shape of the complex reported in panel B. **B.** wings shapes obtained by inverse transformation (black color) superimposed on the mean shape of the complex (red color).

Table 1
Summary of statistics for the analyzed *An. daciae* sp. inq. and *An. maculipennis* s. s.

Species	COI group[a]	Haplotypes[b]	N[c]
An. daciae sp. inq.	A	46	107
	B	31	59
An. maculipennis s.s.	1	25	47
	2	20	33

Note:.
[a] COI group identified by Calzolari et al. (under review);.
[b] number of identified haplotypes;.
[c] number of individuals.

multigenic trait with high hereditability and selective pressures acting on the underline genes may be different from those of the COI (Gilchrist and Partridge, 2001; Hoffmann and Shirriffs, 2002; Moraes et al., 2004; Patterson and Klingenberg, 2007; Henry et al., 2010).

Morphological variation described within haplotype gives interesting results in the framework of phenotypic plasticity, i.e. the ability of a genotype to produce different phenotypes in response to stimuli or inputs from the environment (DeWitt and Scheiner, 2004; West-Eberhard, 2005; Sommer, 2020). Phenotypic plasticity may account for population responses to rapid environmental change or fluctuation and to adaptive tracking on an ecological time scale (Rudman et al., 2022). Within species, regardless of haplotypes, the HDBSCAN unsupervised ML algorithm clustered different morphotypes: 12 in *An. daciae* sp. inq. and 4 in *An. maculipennis* s.s. Each morphotype shared a similar pattern of variation in the subcostal vein, in the anal vein and in the radio medial cross veins of the wing. Interestingly, in the two species *An. daciae* sp. inq. and *An. maculipennis* s.s., there were several similar morphotypes and patterns of variation. At the same time, in the marginal part of the wings, no variation was detected in both species. According to our previous results (Bellin et al., 2021), two coordinates relative to variation in radio medial cross veins (landmarks 15 and 16; Fig. 1), are important in the discrimination between sibling species (Severini et al., 2009; Becker et al., 2010). In many species of Culicidae, landmarks located on the center of the wing showed higher variability (Beriotto et al., 2021). In contrast, landmarks with lower variability were found on the margin of the wing, suggesting that landmarks with aerodynamic restrictions are evolutionarily preserved (Bomphrey et al., 2017). Interestingly, several morphotypes, pattern of variation and morphological stasis were similar in the two species. Morphological

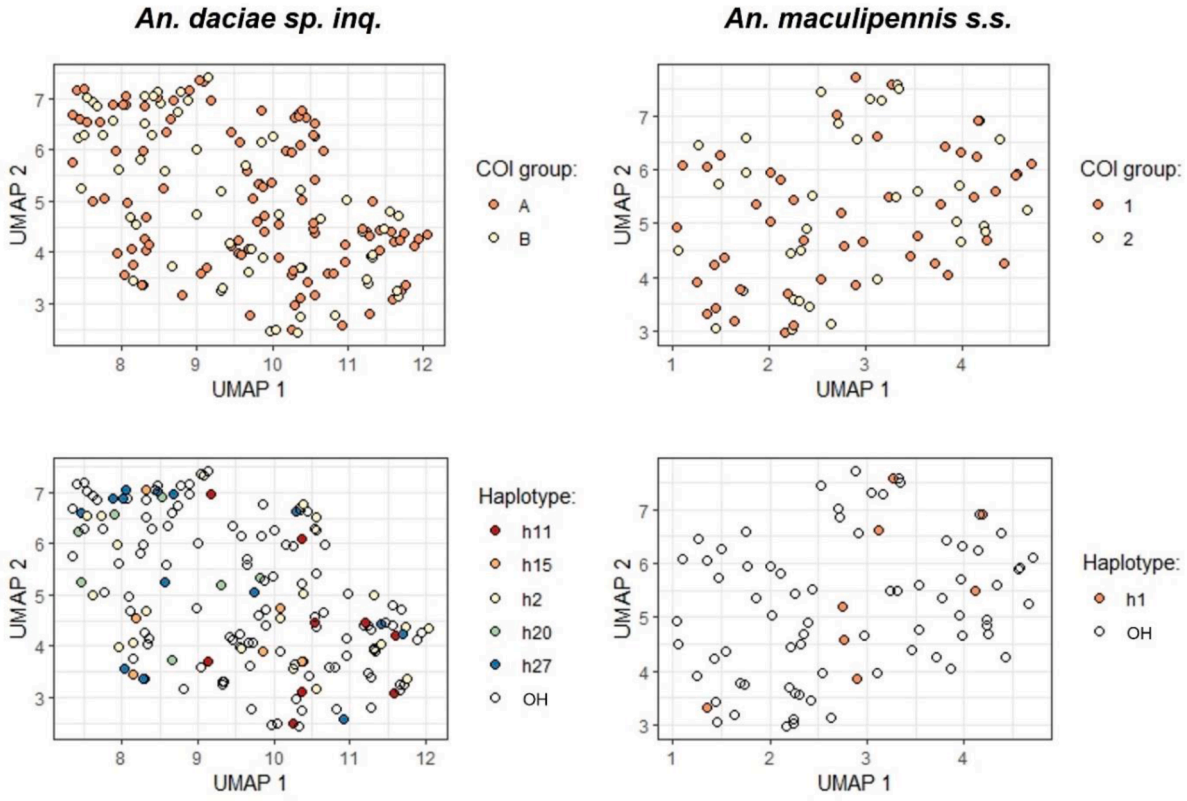

Fig. 3. Superimposition of the COI genetic groups (top panels) and the COI haplotypes (low panels) on the embedding space of UMAP. In low panels OH (others) referred to haplotypes including less than six individuals.

Table 2
PERMANOVA test of shape differences among genetic COI groups with 999 random permutations. For each taxon, the degree of freedom (Df), the sum of squares (SS), the means squared error (MS), the coefficient of determination of the test (Rsq), the F statistic, the effect sizes (Z) and the p-value of the test were reported.

An. daciae sp. inq.		Df	SS	MS	Rsq	F	Z	*p*-value
	COI groups	1	0.0014	0.0014	0.0090	1.4	1.1	0.13
	Residual	164	0.16	0.0009	0.99			
	Total	165	0.16					
An. maculipennis s.s.	COI groups	1	0.00070	0.00070	0.0084	0.6	−0.73	0.75
	Residual	78	0.083	0.0010	0.99			
	Total	79	0.083					

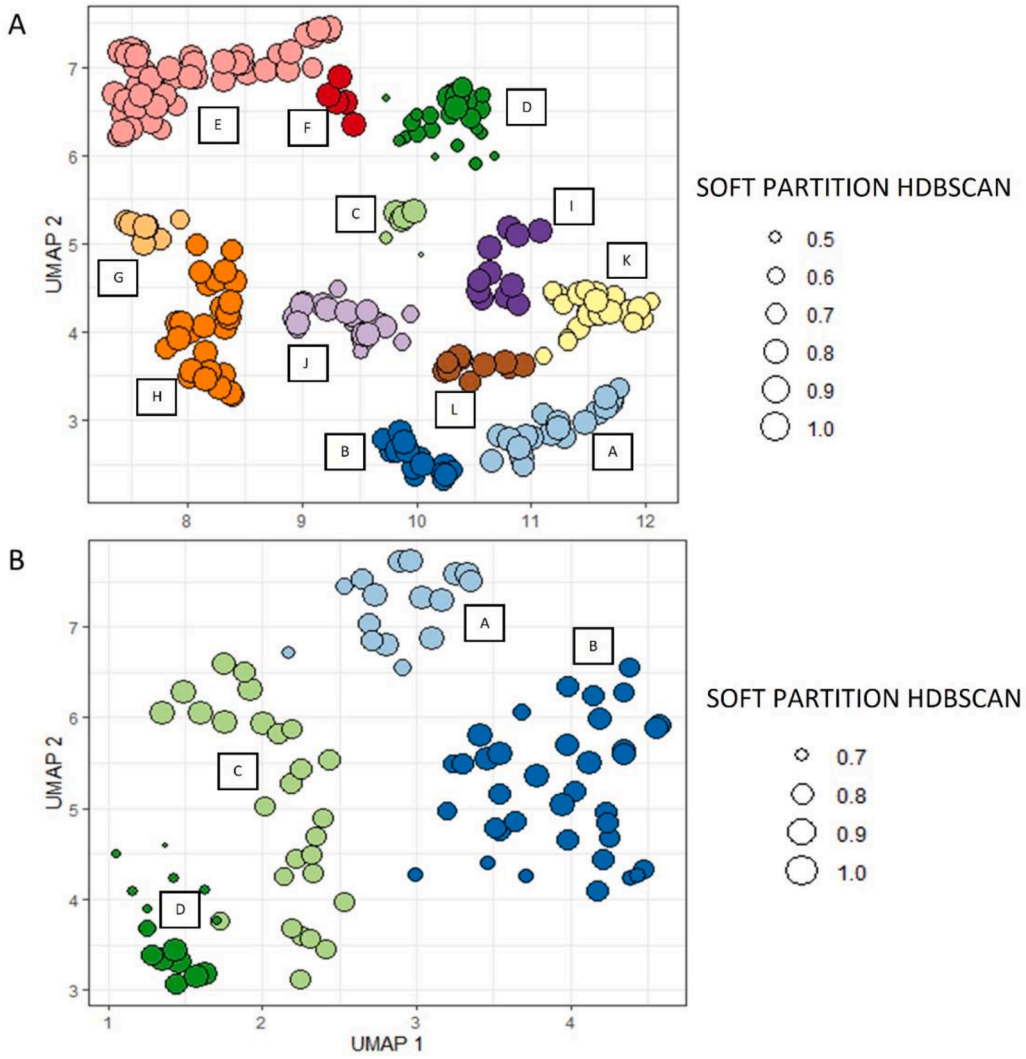

Fig. 4. Panel A (An. daciae sp. inq.) and panel B (An. maculipennis s.s.) reported the result of HDBSCAN algorithm. The colors represented the morphological clusters identified by the algorithm. The size of each point was proportional to the membership values estimated by HDBSCAN. Outliers that are not assigned to the clusters were removed and considered as noise.

similarity and the shape of wing resulting from evolutionary adaptations might be related to various functional roles and responses to selective pressures, or different ontogenetic processes (Zelditch et al., 2006; Aytekin et al., 2007; De Morais et al., 2010). The stasis or variability of a landmark is probably regulated by phylogenetic and functional constraints. As in other insects, the mosquito wings are complex three-dimensional structures that are mainly evolved for locomotion but have several functions under selective pressures (Krishna et al., 2020). The structure and architecture of the veins are crucial for the biomechanical properties of the wings and determine wing deformation during flight (Combes and Daniel, 2003; Appel et al., 2015; Rajabi et al., 2016a; Sun et al., 2021). The veins also enhance the fracture toughness of heavily stressed wings, mitigate collision damage and the tapered shape improves span efficiency during root-flapping (Dirks and Taylor, 2012; Mountcastle and Combes, 2014; Rajabi et al., 2015). The current shape, however, is probably from the sole result of an evolutionary selection process towards maximum aerodynamic performance (Ray et al., 2016). Insect wings generally serve for more than flight; wing-beat frequency, for instance, is important in male and species recognition, territorial or sexual signaling that are fundamental evolutionary requirements affecting the organism's fitness and reproductive isolation in sympatric populations of closely-related mosquito species (Gibson et al., 2010; Chapman et al., 2003). Moreover, insect wings may be involved in other biological functions, such as protection and defense, thermoregulation, self-cleaning and have super-hydrophobic and antimicrobial properties (Byun et al., 2009; Ivanova et al., 2013; Pogodin et al., 2013; Kuitunen et al., 2014; Nguyen et al., 2014; Pass, 2018).

In both *An. daciae* sp. inq. and *An. maculipennis* s.s., the lack of correlation between COI genotype and wing shape and the same spatial-temporal distribution among different morphotypes indicated that they cannot be considered ecotypes (Gildenhard et al., 2019).

The recurrent variations or stasis observed among species and within species may have a phylogenetic and functional origin. Variability among and within sympatric species could be related to environmental factors (e.g. temperature, water scarcity, anthropic action, land use and chemicals). Such factors not only determine the species distribution, habitat suitability and niche dimension but may affect developmental plasticity by altering gene-expression patterns and give rise to polyphenisms (Gilbert, 2001; Rodriguez and Beldade, 2020). The occurrence of genotypes that differ in the amount and direction of plasticity that they are able to express is major mechanism of rapid adaptation and response to environmental and global change (Behera and Nanjundiah, 2004; Fox et al., 2019). Looking ahead, the effect of temperature during egg development on different morphotypes of *An. daciae* sp. inq. and in *An. maculipennis* s.s. could be evaluated (Kingsolver and Buckley, 2017; Rodriguez and Beldade, 2020; Bertola et al., 2022).

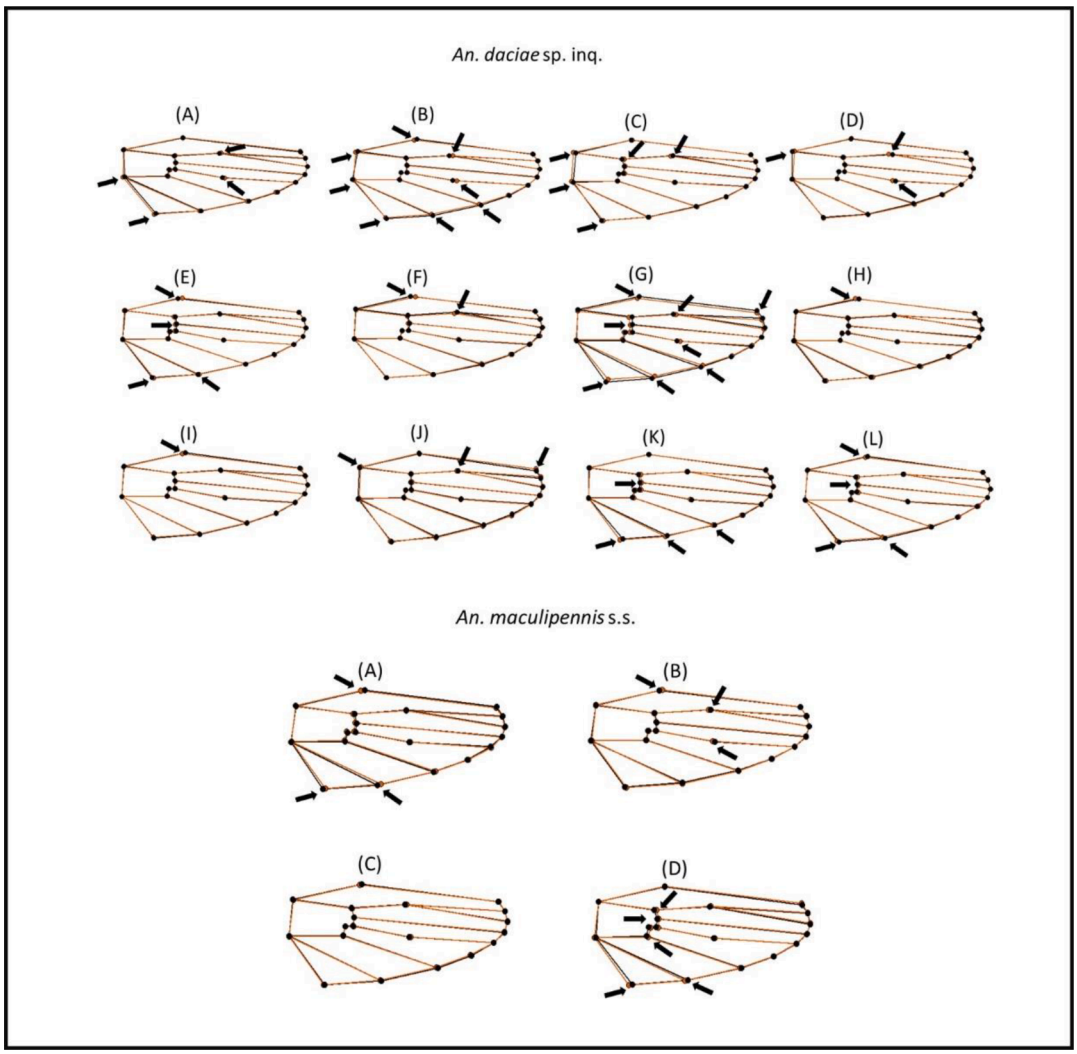

Fig. 5. For each species the mean wing shapes obtained by HDBSCAN clustering (black) was superimposed on the mean shape of the species (red). For each wing, the number referred to the cluster reported in Fig. 3. The arrows indicated the main landmarks variation with the respect to the mean shape of the species.

The use of an instrument to capture images and wingbeat frequency and the analysis of such data by artificial intelligence and deep learning are innovative approaches in biology and ecology (Christin et al., 2019). Convolutional Neural Networks (CNNs) have demonstrated high accuracy in performing image classification tasks, including spectrogram classification (Hershey et al., 2017; Dong et al., 2018). Advances in automated mosquito identification could provide critical tools to monitor mosquito populations and surveillance in real-time (Kim et al., 2021).

Author statement

N.B., M.C, G.M., M.M. and V.R. conceptualized and designed work
M.C., G.M., E.C., P.B., D.L., M.D and M.M. collected data
N.B. and V.R. provided data analysis and interpretation
N.B., M.C., G.M., M.M. and V.R drafted the article
All authors contributed to manuscript writing, critically revised the article and approved the final version to be published.

Declaration of Competing Interest

The Authors declares that there is no conflict of interest.

Acknowledgments

NB was supported by the PhD program in Evolutionary Biology and Ecology (University of Parma, agreement with University of Ferrara and University of Firenze). This research was carried out as part of the 'COMP-HUB' Initiative, funded by the 'Departments of Excellence' Project of the Italian Ministry for Education, University and Research (MIUR) and by the Italian Ministry of Health, PRC "Identification of mosquito species of the Maculipennis Complex through biomolecular and morphometric approaches", code E88C16000190001, IZLER code PRC2015017.

Supplementary materials

Supplementary material associated with this article can be found, in the online version, at doi:10.1016/j.actatropica.2022.106585.

References

Adams, D.C., Collyer, M.L., and Kaliontzopoulou, A. (2020). Geomorph: software for geometric morphometric analyses. R package version 3.2.1. https://doi.org/https://cran.r-project.org/package=geomorph.
Anderson, M.J., 2001. A new method for non-parametric multivariate analysis of variance. Aust. Ecol. 26 (1), 32–46. https://doi.org/10.1111/j.1442-9993.2001.01070.

Appel, E, Heepe, L, Lin, C P, Gorb, S N, 2015. Ultrastructure of dragonfly wing veins: composite structure of fibrous material supplemented by resilin. J. Anat. 227, 561–582. https://doi.org/10.1111/joa.12362.

Artemov, G.N., Fedorova, V.S., Karagodin, D.A., Brusentsov, I.I., Baricheva, E.M., Sharakhov, I.V., Gordeev, M.I., Sharakhova, M.V., 2021. New Cytogenetic Photomap and Molecular Diagnostics for the Cryptic Species of the Malaria Mosquitoes *Anopheles messeae* and *Anopheles daciae* from Eurasia. Insects 12 (9), 835. https://doi.org/10.3390/INSECTS12090835, 2021, Vol. 12, Page 835.

Aytekin, A.M., Alten, B., Caglar, S.S., Ozbel, Y., Kaynas, S., Simsek, F.M., Kasap, O.E., Belen, A., 2007. Phenotypic variation among local populations of phlebotomine sand flies (Diptera: psychodidae) in southern Turkey. J. Vector Ecol. 32 (2), 226.

Bates, D., Mächler, M., Bolker, B.M., Walker, S.C., 2015. Fitting linear mixed-effects models using lme4. J. Stat. Softw. 67 (1), 1–48. https://doi.org/10.18637/JSS.V067.I01.

Becker, N., Petric, D., Zgomba, M., Boase, C., Madon, M.B., Dahl, C., Kaiser, A., 2010. Mosquitoes and Their Control. Springer-Verlag, Berlin Heidelberg.

Begon, M., Townsend, C.R., Harper, J.L., 2006. Ecology: From Individuals to Ecosystems, 4th (Ed.). Blackwell Publishing.

Behera, N., Nanjundiah, V., 2004. Phenotypic plasticity can potentiate rapid evolutionary change. J. Theor. Biol. 226 (2), 177–184. https://doi.org/10.1016/j.jtbi.2003.08.011.

Bellin, N., Calzolari, M., Callegari, E., Bonilauri, P., Grisendi, A., Dottori, M., Rossi, V., 2021. Geometric morphometrics and machine learning as tools for the identification of sibling mosquito species of the Maculipennis complex (*Anopheles*). Infect. Genet. Evol. 95 (August) https://doi.org/10.1016/j.meegid.2021.105034.

Beriotto, A.C., Garzón, M.J., Schweigmann, N., 2021. Is there a minimum number of landmarks that optimizes the geometric morphometric analysis of mosquito (Diptera, Culicidae) wings? J. Med. Entomol. 58 (2), 576–587. https://doi.org/10.1093/jme/tjaa187.

Bertola, M., Mazzucato, M., Pombi, M., Montarsi, F., 2022. Updated occurrence and bionomics of potential malaria vectors in Europe: a systematic review (2000–2021). Parasites Vectors 15, 88. https://doi.org/10.1186/s13071-022-05204-y.

Bomphrey, R.J., Nakata, T., Phillips, N., Walker, S.M., 2017. Smart wing rotation and trailing-edge vortices enable high frequency mosquito flight. Nature 544 (7648), 92–95. https://doi.org/10.1038/nature21727.

Bookstein, F.L., 1991. Morphometric Tools for Landmark Data. Cambridge University Press. https://doi.org/10.1017/CBO9780511573064.

Bookstein, F.L., 1996. Combining the tools of geometric morphometrics. Adv. Morphometrics 131–151. https://doi.org/10.1007/978-1-4757-9083-2_12.

Byun, D., Hong, J., Saputra, Ko, J.H., Lee, Y.J., Park, H.C., Byun, B.K., Lukes, J.R, 2009. Wetting characteristics of insect wing surfaces. J. Bionic Eng. 6 (1), 63–70. https://doi.org/10.1016/S1672-6529(08)60092-X.

Brunetti, M., Magoga, G., Iannella, M., Biondi, M., Montagna, M., 2019. Phylogeography and species distribution modelling of *Cryptocephalusbarii* (Coleoptera: chrysomelidae): is this alpine endemic species close to extinction? Zookeys 856, 3–25. https://doi.org/10.3897/zookeys.856.32462.

Calzolari, M., Desiato, R., Albieri, A., Bellavia, V., Bertola, M., Bonilauri, P., Callegari, E., Canziani, S., Lelli, D., Mosca, A., Mulatti, P., Peletto, S., Ravagnan, S., Roberto, P., Torri, D., Pombi, M., Di Luca, M., Montarsi, F., 2021. Mosquitoes of the maculipennis complex in Northern Italy. Sci. Rep. 11 (1), 1–12. https://doi.org/10.1038/s41598-021-85442-9.

Campello, R.J.G.B., Moulavi, D., Sander, J, 2013. Density-based clustering based on hierarchical density estimates. In: Pei, J., Tseng, V.S., Cao, L., Motoda, H., Xu, G. (Eds.), Advances in Knowledge Discovery and Data Mining. PAKDD 2013. Lecture Notes in Computer Science. Springer, Berlin, Heidelberg. https://doi.org/10.1007/978-3-642-37456-2_14 vol 7819.

Chapman, H.F., Hughes, J.M., Ritchie, S.A., Kay, B.H., 2003. Population structure and dispersal of the freshwater mosquitoes *Culex annulirostris* and *Culex palpalis* (Diptera: culicidae) in Papua New Guinea and Northern Australia. J. Med. Entomol. 40 (2), 165–169. https://doi.org/10.1603/0022-2585-40.2.165.

Christin, S., Hervet, É., Lecomte, N., 2019. Applications for deep learning in ecology. Methods Ecol. Evol. 10 (10), 1632–1644. https://doi.org/10.1111/2041-210X.13256.

Combes, S.A., Daniel, T.L., 2003. Flexural stiffness in insect wings II. Spatial distribution and dynamic wing bending. J. Exp. Biol. 206 (17), 2989–2997. https://doi.org/10.1242/JEB.00524.

De Morais, S.A., Moratore, C., Suesdek, L., Marrelli, M.T., 2010. Genetic-morphometric variation in *Culex quinquefasciatus* from Brazil and La Plata, Argentina. Mem. Inst. Oswaldo Cruz 105 (5), 672–676. https://doi.org/10.1590/s0074-02762010000500012.

DeWitt, T.J., Scheiner, S.M., 2004. Phenotypic Plasticity: Functional and Conceptual Approaches. Oxford University Press, New York.

Diaz-Papkovich, A., Anderson-Trocmé, L., Ben-Eghan, C., Gravel, S., 2019. UMAP reveals cryptic population structure and phenotype heterogeneity in large genomic cohorts. PLoS Genet. 15 (11), e1008432 https://doi.org/10.1371/JOURNAL.PGEN.1008432.

Dirks, J.H., Taylor, D., 2012. Veins improve fracture toughness of insect wings. PLoS One 7 (8), e43411. https://doi.org/10.1371/JOURNAL.PONE.0043411.

Dong, X., Yan, N., Wei, Y., 2018. Insect sound recognition based on convolutional neural network. In: 3rd IEEE International Conference on Image, Vision and Computing, ICIVC, pp. 855–859. https://doi.org/10.1109/ICIVC.2018.8492871.

Doorenweerd, C., San Jose, M., Barr, N., Leblanc, L., Rubinoff, D., 2020. Highly variable COI haplotype diversity between three species of invasive pest fruit fly reflects remarkably incongruent demographic histories. Sci. Rep. 10, 6887. https://doi.org/10.1038/s41598-020-63973-x.

Dorrity, M.W., Saunders, L.M., Queitsch, C., Fields, S., Trapnell, C., 2020. Dimensionality reduction by UMAP to visualize physical and genetic interactions. Nat. Commun. 11 (1), 1–6. https://doi.org/10.1038/s41467-020-15351-4, 2020 11:1.

Edgar, R.C., 2004. MUSCLE: a multiple sequence alignment method with reduced time and space complexity. BMC Bioinform. 5, 113.

Fox, R.J., Donelson, J.M., Schunter, C., Ravasi, T., Gaitán-Espitia, J.D., 2019. Beyond buying time: the role of plasticity in phenotypic adaptation to rapid environmental change. Philos. Trans. R. Soc. Lond. B Biol. Sci. 374 (1768) https://doi.org/10.1098/RSTB.2018.0174.

Francuski, L., Gojković, N., Krtinić, B., Milankov, V., 2019. The diagnostic utility of sequence-based assays for the molecular delimitation of the epidemiologically relevant *Culex pipiens pipiens* taxa (Diptera: culicidae). Bull. Entomol. Res. 109 (6), 752–761. https://doi.org/10.1017/S0007485319000105.

Gibson, G, Warren, B, Russell, I J, 2010. Humming in Tune: Sex and Species Recognition by Mosquitoes on the Wing. JARO 11, 527–540. https://doi.org/10.1007/s10162-010-0243-2.

Gilchrist, A.S., Partridge, L., 2001. The contrasting genetic architecture of wing size and shape in *Drosophila melanogaster*. Heredity (Edinb) 86 (2), 144–152. https://doi.org/10.1046/j.1365-2540.2001.00779.x.

Gildenhard, M., Rono, E.K., Diarra, A., Boissière, A., Bascunan, P., Carrillo-Bustamante, P., Camara, D., Krüger, H., Mariko, M., Mariko, R., Mireji, P., Nsango, S. E., Pompon, J., Reis, Y., Rono, M.K., Seda, P.B., Thailayil, J., Traorè, A., Yapto, C.V., Awono-Ambene, P., Dabiré, R.K., Diabaté, A., Masiga, D., Catteruccia, F., Morlais, I., Diallo, M., Sangare, D., Levashina, E.A., 2019. Mosquito microevolution drives *Plasmodium falciparum* dynamics. Nat. Microbiol. 4 (6), 941–947. https://doi.org/10.1038/s41564-019-0414-9, 2019 4:6.

Goodal, C., 1991. Procrustes methods in the statistical analysis of shape. J. R. Stat. Soc. Ser. C 53 (2), 285–339. https://www.jstor.org/stable/2345744?seq=1.

Henry, A., Thongsripong, P., Fonseca-Gonzalez, I., Jaramillo-Ocampo, N., Dujardin, J.P., 2010. Wing shape of dengue vectors from around the world. Infect. Genet. Evol. 10 (2), 207–214. https://doi.org/10.1016/j.meegid.2009.12.001.

Hershey, S., Chaudhuri, S., Ellis, D.P.W., Gemmeke, J.F., Jansen, A., Moore, R.C., Plakal, M., Platt, D., Saurous, R.A., Seybold, B., Slaney, M., Weiss, R.J., Wilson, K., 2017. CNN architectures for large-scale audio classification. In: ICASSP, IEEE International Conference on Acoustics, Speech and Signal Processing - Proceedings, pp. 131–135. https://doi.org/10.1109/ICASSP.2017.7952132.

Hoffmann, A.A., Shirriffs, J., 2002. Geographic variation for wing shape in *Drosophila serrata*. Evolution (N Y) 56 (5), 1068–1073. https://doi.org/10.1111/j.0014-3820.2002.tb01418.x.

Ivanova, E.P., Hasan, J., Webb, H.K., Gervinskas, G., Juodkazis, S., Truong, V.K., Wu, A. H.F., Lamb, R.N., Baulin, V.A., Watson, G.S., Watson, J.A., Mainwaring, D.E., Crawford, R.J., 2013. Bactericidal activity of black silicon. Nat. Commun. 4 (1), 1–7. https://doi.org/10.1038/ncomms3838.

Kareemi, T.I., Nirankar, J.K., Mishra, A.K., Chand, S.K., Chand, G., Vishwakarma, A.K., Tiwari, A., Bharti, P.K., 2021. Population dynamics and insecticide susceptibility of *Anopheles culicifacies* in Malaria endemic districts of Chhattisgarh, India. Insects 12 (4), 284. https://doi.org/10.3390/INSECTS12040284, 2021, Vol. 12, Page 284.

Kim, D., DeBriere, T.J., Cherukumalli, S., White, G.S., Burkett-Cadena, N.D., 2021. Infrared light sensors permit rapid recording of wingbeat frequency and bioacoustic species identification of mosquitoes. Sci. Rep. 11 (1), 1–9. https://doi.org/10.1038/s41598-021-89644-z, 2021 11:1.

Kimura, M.A., 1980. Simple method for estimating evolutionary rates of base substitutions through comparative studies of nucleotide sequences. J. Mol. Evol. 16, 111–120.

Kingsolver, J.G., Buckley, L.B., 2017. Quantifying thermal extremes and biological variation to predict evolutionary responses to changing climate. Philos. Trans. Royal Soc. B 372 (1723). https://doi.org/10.1098/RSTB.2016.0147.

Klingenberg, C.P., 2013. Visualizations in geometric morphometrics: how to read and how to make graphs showing shape changes. Hystrix, Italian J. Mammal. 24 (1), 15–24. https://doi.org/10.4404/HYSTRIX-24.1-7691.

Krishna, S., Cho, M., Wehmann, H.N., Engels, T., Lehmann, F.O., 2020. Wing design in flies: properties and aerodynamic function. Insects 11 (8), 466. https://doi.org/10.3390/insects11080466.

Kuitunen, K., Kovalev, A., Gorb, S.N., 2014. Sex-related effects in the superhydrophobic properties of damselfly wings in young and old *Calopteryx splendens*. PLoS One 9 (2), e88627. https://doi.org/10.1371/JOURNAL.PONE.0088627.

Lilja, T., Eklöf, D., Jaenson, T.G.T., Lindström, A., Terenius, O., 2020. Single nucleotide polymorphism analysis of the ITS2 region of two sympatric malaria mosquito species in Sweden: *anopheles daciae* and *Anopheles messeae*. Med. Vet. Entomol. 34 (3), 364–368. https://doi.org/10.1111/mve.12436.

Lorenz, C., Marques, T.C., Sallum, M.A.M., Suesdek, L., 2012. Morphometrical diagnosis of the malaria vectors *Anopheles cruzii, An. homunculus* and *An. bellator*. Parasites Vectors 5 (1), 2–8. https://doi.org/10.1186/1756-3305-5-257.

Lorenz, C., Ferraudo, A.S., Suesdek, L., 2015a. Artificial neural network applied as a methodology of mosquito species identification. Acta Trop. 152, 165–169. https://doi.org/10.1016/j.actatropica.2015.09.011.

Lorenz, C., Patané, J.S.L., Suesdek, L., 2015b. Morphogenetic characterisation, date of divergence, and evolutionary relationships of malaria vectors *Anopheles cruzii* and *Anopheles homunculus*. Infect. Genet. Evol. 35, 144–152. https://doi.org/10.1016/j.meegid.2015.08.011.

Magoga, G., Fontaneto, D., Montagna, M., 2021. Factors affecting the efficiency of molecular species delimitation in a species-rich insect family. Mol. Ecol. Resour. 21 (5), 1475–1489. https://doi.org/10.1111/1755-0998.13352.

Magoga, G., Sahin, D.C., Fontaneto, D., Montagna, M., 2018. Barcoding of Chrysomelidae of Euro-Mediterranean area: efficiency and problematic species. Sci. Rep. 8 (1), 13398. https://doi.org/10.1038/s41598-018-31545-9.

Manguin, S., Bangs, M.J., Pothikasikorn, J., Chareonviriyaphap, T., 2010. Review on global co-transmission of human *Plasmodium* species and *Wuchereria bancrofti* by *Anopheles* mosquitoes. Infection. Genet. Evol. 10 (2), 159–177. https://doi.org/10.1016/j.meegid.2009.11.014.

Manguin, S., Garros, C., Dusfour, I., Harbach, R.E., Coosemans, M., 2008. Bionomics, taxonomy, and distribution of the major malaria vector taxa of *Anopheles* subgenus Cellia in Southeast Asia: an updated review. Infection, Genet. Evol. 8 (4), 489–503. https://doi.org/10.1016/j.meegid.2007.11.004.

McInnes, L., Healy, J., and Melville, J. (2018). UMAP: uniform Manifold Approximation and Projection for Dimension Reduction. http://arxiv.org/abs/1802.03426.

Moraes, E.M., Manfrin, M.H., Laus, A.C., Rosada, R.S., Bomfin, S.C., Sene, F.M., 2004. Wing shape heritability and morphological divergence of the sibling species *Drosophila mercatorum* and Drosophila paranaensis. Heredity (Edinb) 92 (5), 466–473. https://doi.org/10.1038/sj.hdy.6800442, 2004 92:5.

Moulavi, D., Jaskowiak, P.A., Campello, R.J.G.B., Zimek, A., Sander, J., 2014. Density-based clustering validation. In: Proceedings of the 14th SIAM International Conference on Data Mining (SDM). Philadelphia, PA.

Mountcastle, A.M., Combes, S.A., 2014. Biomechanical strategies for mitigating collision damage in insect wings: structural design versus embedded elastic materials. J. Exp. Biol. 217 (Pt 7), 1108–1115. https://doi.org/10.1242/JEB.092916.

Nguyen, S.H., Webb, H.K., Mahon, P.J., Crawford, R.J., Ivanova, E.P., 2014. Natural insect and plant micro-/nanostructsured surfaces: an excellent selection of valuable templates with superhydrophobic and self-cleaning properties. Molecules 19 (9), 13614–13630. https://doi.org/10.3390/MOLECULES190913614, 2014, Vol. 19, Pages 13614-13630.

Nicolescu, G., Linton, Y.-.M., Vladimirescu, A., Howard, T.M., Harbach, R.E., 2004. Mosquitoes of the Anopheles maculipennis group (Diptera: culicidae) in Romania, with the discovery and formal recognition of a new species based on molecular and morphological evidence. Bull. Entomol. Res. 94 (6), 525–535. https://doi.org/10.1079/ber2004330.

Pass, G., 2018. Beyond aerodynamics: the critical roles of the circulatory and tracheal systems in maintaining insect wing functionality. Arthropod. Struct. Dev. 47 (4), 391–407. https://doi.org/10.1016/J.ASD.2018.05.004.

Patterson, J.S., Klingenberg, C.P., 2007. Developmental buffering: how many genes? Evol. Dev. 9 (6), 525–526. https://doi.org/10.1111/j.1525-142X.2007.00193.x.

Pfenninger, M., Schwenk, K., 2007. Cryptic animal species are homogeneously distributed among taxa and biogeographical regions. BMC Evol. Biol. 7 (1), 1–6. https://doi.org/10.1186/1471-2148-7-121/TABLES/2.

Pogodin, S., Hasan, J., Baulin, V.A., Webb, H.K., Truong, V.K., Phong Nguyen, T.H., Boshkovikj, V., Fluke, C.J., Watson, G.S., Watson, J.A., Crawford, R.J., Ivanova, E.P., 2013. Biophysical model of bacterial cell interactions with nanopatterned cicada wing surfaces. Biophys. J. 104 (4), 835–840. https://doi.org/10.1016/J.BPJ.2012.12.046.

Popescu, A.A., Huber, K.T., Paradis, E., 2012. Ape 3.0: new tools for distance based phylogenetics and evolutionary analysis in R. Bioinformatics 28, 1536–1537.

Core Team, R., 2019. R: A language and Environment For Statistical Computing. R Foundation for Statistical Computing, Vienna, Austria. URL. https://www.r-project.org/.

Rajabi, H., Darvizeh, A., Shafiei, A., Taylor, D., Dirks, J.H., 2015. Numerical investigation of insect wing fracture behaviour. J. Biomech. 48 (1), 89–94. https://doi.org/10.1016/J.JBIOMECH.2014.10.037.

Rajabi, H, Shafiei, A, Darvizeh, A, Dirks, J H, Appel, E, Gorb, S N, 2016a. Effect of microstructure on the mechanical and damping behaviour of dragonfly wing veins. R. Soc. Open Sci. 3 (160006) https://doi.org/10.1098/rsos.160006.

Ray, R, Nakata, T, Henningsson, P, Bomphrey, R J, 2016. Enhanced flight performance by genetic manipulation of wing shape in *Drosophila*. Nat. Commun. 7 (10851) https://doi.org/10.1038/ncomms10851.

Rodrigues, Y.K., Beldade, P., 2020. Thermal plasticity in insects' response to climate change and to multifactorial environments. Front. Ecol. Evol. 8, 271. https://doi.org/10.3389/FEVO.2020.00271/BIBTEX.

Rudman, S.M., Greenblum, S.I., Rajpurohit, S., Betancourt, N.J., Hanna, J., Tilk, S., Yokoyama, T., Petrov, D.A., Schmidt, P., 2022. Direct observation of adaptive tracking on ecological time scales in *Drosophila*. Science. https://doi.org/10.1126/SCIENCE.ABJ7484.

Severini, F., Toma, L., Di Luca, M., Romi, R., 2009. Le Zanzare Italiane: generalità E Identificazione Degli Adulti (Diptera, Culicidae). Fragmenta Entomol. 41 (2), 213. https://doi.org/10.4081/fe.2009.92.

Shannon, C.E., Wiener, W., 1963. The Mathematical Theory of Communication. University of Illinois Press.

Sommer, R.J., 2020. Phenotypic plasticity: from theory and genetics to current and future challenges. Genetics, 215 (1), 1–13. https://doi.org/10.1534/GENETICS.120.303163.

Sun, J.Y., Yan, Y.W., Li, F.D., Zhang, Z.J., 2021. Generative design of bioinspired wings based on deployable hindwings of *Anomala Corpulenta* Motschulsky. Micron 151, 103150. https://doi.org/10.1016/J.MICRON.2021.103150.

Tatsuta, H., Takahashi, K.H., Sakamaki, Y., 2018. Geometric morphometrics in entomology: basics and applications. Entomol. Sci. 21 (2), 164–184. https://doi.org/10.1111/ens.12293.

Vrijenhoek, R.C., Johnson, S.B., Rouse, G.W., 2009. A remarkable diversity of bone-eating worms (Osedax; Siboglinidae; Annelida). BMC Biol. 7 (1), 1–13. https://doi.org/10.1186/1741-7007-7-74/TABLES/4.

West-Eberhard, M.J., 2005. Developmental plasticity and the origin of species differences. Proc. Natl. Acad. Sci. U. S. A. 102 (SUPPL. 1), 6543–6549. https://doi.org/10.1073/PNAS.0501844102.

Wilke, A.B.B., de Oliveira Christe, R., Multini, L.C., Vidal, P.O., Wilk-Da-silva, R., de Carvalho, G.C., Marrelli, M.T., 2016. Morphometric wing characters as a tool for mosquito identification. PLoS One 11 (8), 1–12. https://doi.org/10.1371/journal.pone.0161643.

Yang, Y., Sun, H., Zhang, Y., Zhang, T., Gong, J., Wei, Y., Duan, Y.G., Shu, M., Yang, Y., Wu, D., Yu, D., 2021. Dimensionality reduction by UMAP reinforces sample heterogeneity analysis in bulk transcriptomic data. Cell Rep. 36 (4), 109442 https://doi.org/10.1016/J.CELREP.2021.109442.

Zelditch, M.L., Mezey, J., Sheets, H.D., Lundrigan, B.L., Garland, T., 2006. Developmental regulation of skull morphology II: ontogenetic dynamics of covariance. Evol. Dev. 8 (1), 46–60. https://doi.org/10.1111/j.1525-142X.2006.05074.x.

Zheng, J.H., Nie, H.T., Yang, F., Xi-Wu, J., 2019. Genetic variation and population structure of different geographical populations of Meretrix petechialis based on mitochondrial gene COI. J. Genet. 98, 68. https://doi.org/10.1007/s12041-019-1111-4.